X-ray Crystal Structures and ab Initio Calculations on the Photochemically Formed Dewar Isomers of the 4(3*H*)-Pyrimidinone Derivatives

Shun-ichi Hirokami,* Akihiro Murao, and Hiroko Kakuda

Laboratory of Chemistry, Toyama Medical and Pharmaceutical University, Sugitani 2630, Toyama 930-01, Japan

Hiroyuki Shinoda

Faculty of Pharmaceutical Sciences, Toyama Medical and Pharmaceutical University, Sugitani 2630, Toyama 930-01, Japan

Yoshinori Koga

Department of Advanced Chemical Technology, National Institute of Materials and Chemical Research, 1-1, Higashi, Tsukuba, Ibaraki 305, Japan

Received November 11, 1996[⊗]

The structures of the 5-oxo-2,6-diazabicyclo[2.2.0]hex-2-enes (imine Dewar pyrimidinones) **2a**−**h** have been studied by X-ray diffraction analysis and ab initio calculations at the HF/6-31G(d,p) and MP2/6-31G(d,p) levels of theory. The crystal structures of 1-alkyl-3-*tert*-butyl-6-methyl imine Dewar pyrimidinones **2a**−**c** have been determined at low temperature. The X-ray diffraction studies revealed that both the 2-azetidinone and dihydroazete rings are almost planar, and their eight bond angles are nearly 90° (81−100°). The C1−N2(=C3) bond distance in the dihydroazete ring is longer due to the bond angle strain by ca. 0.06 Å than that of a typical straight-chain imine molecule. Full geometry optimizations on the imine Dewar isomers (**2a** and **2d**−**h**) show deviations between the HF and MP2 geometries. The MP2 structure of the 3-*tert*-butyl-1,6-dimethyl imine Dewar pyrimidinone **2a** is compared with those of the X-ray diffraction. The results of the calculations are found to be in good agreement with the X-ray diffraction data. The full geometry optimizations are necessary with the inclusion of electron correlation for the highly strained molecules. The ab initio calculations of the 2-azetidinone **9**, 3,4-dihydroazete **11**, and *N*-ethylidenemethylamine **12** have been carried out at the HF and MP2/6-31G(d,p) levels of theory to compare with the structures, orbital hybridization, bond orders, and charge distributions of the Dewar pyrimidinones **2**. The theoretical results reveal that the MP2 C1−N2 bond distance of the Dewar pyrimidinone **2a** is consistent with the abnormally elongated X-ray C1−N2 bond distance. The electronegative N2 and N6 atoms in the Dewar pyrimidinones **2** give the great positive charge on the C1 atom. The smaller bond angles (ca. 90°) in the Dewars **2** than typical sp^2 and sp^3 bond angles (ca. 120 and 109°) increase p character in the endocyclic bonds and decrease p character in the exocyclic bonds.

Introduction

The photolysis of 2,3,6-trialkyl-4(3*H*)-pyrimidinones **1** undergoes a variety of reactions in protic solvents (alcohol, carboxylic acid, amine, and water).[1] The typical photochemical reactions are shown in Figure 1. The reactive and unstable photochemical intermediates are the valence-bond isomers (Dewar pyrimidinones) **2**, which react with the protic solvent molecules to give the 4-methoxy-2-azetidinone **3** in methanol, pyrimidinium-5-carboxylate **4** in acetic acid, imine **5** in methylamine, and enamide **6** in water or aqueous solution. However,

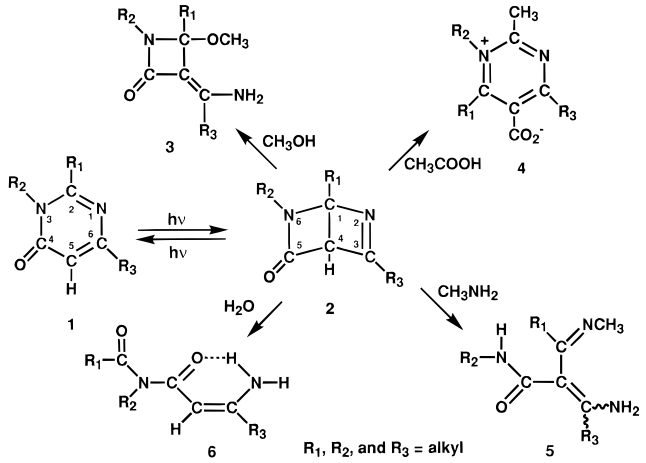

Figure 1. The photochemical and thermal reaction scheme of the 2,3,6-trialkyl-4-pyrimidinone **1** and Dewar pyrimidinone **2**.

⊗ Abstract published in *Advance ACS Abstracts,* April 15, 1997.

(1) (a) Hirokami, S.; Hirai, Y.; Nagata, M.; Yamazaki, T.; Date, T. *J. Org. Chem.* **1979**, *44*, 2083−2087. (b) Hirai, Y.; Yamazaki, T.; Hirokami, S.; Nagata, M. *Tetrahedron Lett.* **1980**, *21*, 3067−3070. (c) Hirokami, S.; Takahashi, T.; Nagata, M.; Hirai, Y.; Yamazaki, T. *J. Org. Chem.* **1981**, *46*, 1769−1777. (d) Takahashi, T.; Hirokami, S.; Kato, K.; Nagata, M.; Yamazaki, T. *J. Org. Chem.* **1983**, *48*, 2914−2920. (e) Hirokami, S.; Takahashi, T.; Nagata, M.; Yamazaki, T. *Tetrahedron Lett.* **1983**, *24*, 5237−5240. (f) Hirokami, S.; Takahashi, T.; Kurosawa, K.; Nagata, M.; Yamazaki, T. *J. Org. Chem.* **1985**, *50*, 166−169. (g) Takahashi, T.; Hirokami, S.; Nagata, M.; Yamazaki, T. *Tetrahedron Lett.* **1985**, *26*, 3247−3250. (h) Hirokami, S.; Takahashi, T.; Nagata, M.; Yamazaki, T. *J. Org. Chem.* **1987**, *52*, 2455−2468. (i) Takahashi, T.; Hirokami, S.; Nagata, M.; Yamazaki, T. *J. Chem. Soc., Perkin Trans. 1* **1988**, 2653−2662. (j) Takahashi, T.; Hirokami, S.; Nagata, M.; Yamazaki, T.; Date, T. *J. Chem. Soc., Perkin Trans. 1* **1989**, 1231−1239. (k) Kakuda, H.; Takahashi, Y.; Hirokami, S. *Acta Crystallogr.* **1995**, *C51*, 2647−2650. We have successfully established the structures of the (*E*)- and (*Z*)-1,6-dimethyl enamine Dewar isomers by single crystal X-ray diffraction analysis. The comparison between the enamine Dewar and imine Dewar structures will be reported in the near future.

S0022-3263(96)02103-2 CCC: $14.00

irradiation of the 3-methyl-, 2,3-dimethyl-, and 3,6-dimethyl-4(3*H*)-pyrimidinones in methanol did not give the expected 4-methoxy-2-azetidinone **3**, but, rather, a variety of the degradation products formed by the reactions of the labile imine Dewar pyrimidinones **2** with solvent methanol.[1a,d] The reactions of the Dewar pyrimidinones **2** depend strongly upon the substituents at the 1, 3, and 6 positions.

A good example of the reaction is found with 3-*tert*-butyl-1,6-dimethyl Dewar isomer **2a** in methanol solution. The Dewar isomer gives *N*-methyl-3-(1-amino-2,2-dimethylpropylidene)-4-methoxy-4-methyl-2-azetidinone (**3a**) in a quantitative yield (94%).[1f] This indicates that the solvent molecules as nucleophiles attack neither at the imine C=N bond nor at the amide N−C(=O) bond. The initial step in methanol may involve an ionic cleavage of the C1−N2(=C3) bond by transfer of proton to the N2 atom from the solvent molecules to give an azetidinyl cation, followed by addition of methanol molecule.[1a,h] At the present time, we assume that the ionic cleavage in the C1−N2 bond takes place also in carboxylic acid, amine, and water. The C1−N2 bond may be polarized into the cationic carbon ($C1^+$) and anionic nitrogen ($N2^-$) atoms and is probably lengthened to release the dihydroazete ring strain. The elongation and charge separation of the C1−N2 bond of the dihydroazete ring in the Dewar pyrimidinones **2** can be tested by determination of the structures and by quantum chemical calculations. With this prospect in mind, we have now undertaken the X-ray crystal structural analysis and ab initio molecular orbital calculations of the imine Dewar pyrimidinones **2.** No experimental structure data on the Dewar Pyrimidinones, 3,4-dihydroazete, and their derivatives was reported in the literature**.**

Recently, Lapinski et al. have reported the IR detection of the labile and inseparable Dewar isomers formed by UV photolysis of the 3-methyl-, 6-methyl-, and 2,6-dimethyl-4(3*H*)-pyrimidinones in argon matrix at cryogenic temperature.[2] The structural identification of the product (*N*-methyl Dewar isomer) was established by comparison with the experimental IR spectrum and ab initio vibrational frequencies calculated at the HF/6-31G-(d,p) and MP2/6-31G(d,p) levels of theory. As pointed out by Lapinski et al., the MP2 level calculations are important since remarkable agreement between the experimental and theoretical results was found when electron correlation is included.[2c]

We have recently succeeded in the isolation of the unstable and reactive 1,6-dialkyl-3-*tert*-butyl-5-oxo-2,6-diazabicyclo[2.2.0]hex-2-enes (imine Dewar pyrimidinones)[1f] and (*E*)- and (*Z*)-3-[(alkoxycarbonyl)methylene]-2,6-diazabicyclo[2.2.0]hexan-5-ones (enamine Dewar pyrimidinones)[1f,k] in crystalline form. We report here the X-ray diffraction structures of the three imine Dewar pyrimidinones **2a**−**c** and results of the ab initio molecular orbital calculations on the six imine Dewar pyrimidinones **2a** and **2d**−**h**, 2-azetidinone **9**, 3,4-dihydroazete **11**, and straight-chain imines **12** at the HF/6-31G(d,p) and MP2/6-31G(d,p) levels of theory in order to elucidate the structures, orbital hybridization, bond order, and charge distributions of the substituted Dewar pyrimidinone derivatives.

(2) (a) Nowak, M. J.; Fulara, J.; Lapinski, L. *J. Mol. Struct.* **1988**, *175*, 91−96. (b) Lapinski, L.; Fulara, J.; Nowak, M. *J. Spectrochim. Acta* **1990**, *46A*, 61−71. (c) Lapinski, L.; Nowak, M. J.; Les, A.; Adamowicz, L. *J. Am. Chem. Soc.* **1994**, *116*, 1461−1467.

Experimental Section

Materials. 6-*tert*-Butyl-2,3-dimethyl-4(3*H*)-pyrimidinone (**1a**), 2-benzyl-6-*tert*-butyl-3-methyl-4(3*H*)-pyrimidinone (**1b**), and 6-*tert*-butyl-3-methyl-2-(4-methylbenzyl)-4(3*H*)-pyrimidinone (**1c**) were prepared from iodomethane and 6-*tert*-butyl-2-methyl-4(3*H*)-pyrimidinone, 2-benzyl-6-*tert*-butyl-4(3*H*)-pyrimidinone, and 6-*tert*-butyl-2-(4-methylbenzyl)-4(3*H*)-pyrimidinone in alcoholic solutions containing base at 65−80 °C. The starting 4(3*H*)-pyrimidinones were synthesized from the corresponding amidines and *β*-keto esters.[1f,h]

General Procedure for Preparation of Dewar Pyrimidinones 2. The 4-pyrimidinone (2.0−2.2 g) was dissolved in 300 mL of 2-propanol containing NH_3 (14−19 g) at −20 to −30 °C in a reaction cell. The solution was irradiated for about 6 h under an argon atmosphere with a Nikko Seiki 100-W high-pressure mercury lamp. After irradiation, the solvent was evaporated under vacuum at 20−25 °C, and the reaction mixture was chromatographed on Sephadex LH-20 with chloroform−hexane (4:1 v/v, each fraction 10 mL) as an eluant. The purification, crystallization, and properties of 3-*tert*-butyl-1,6-dimethyl-5-oxo-2,6-diazabicyclo[2.2.0]hex-2-ene (**2a**), 1-benzyl-3-*tert*-butyl-6-methyl-5-oxo-2,6-diazabicyclo[2.2.0]hex-2-ene (**2b**), and 3-*tert*-butyl-6-methyl-1-(4-methylbenzyl)-5-oxo-2,6-diazabicyclo[2.2.0]hex-2-ene (**2c**) are described in the previous papers.[1f,h]

Single Crystals. Colorless prismatic crystals of **2a** suitable for X-ray analysis were gradually grown by crystallization after evaporation of chloroform−hexane solvent under vacuum at 15−20 °C. Colorless prismatic crystals of **2b** and **2c** were obtained by recrystallization from CCl_4−*n*-pentane solution at 10−15 °C.

X-ray Data Collection, Reduction, and Structure Solution. A suitable fragment was cleaved and mounted in a 0.7 mm X-ray glass capillary tube filled with 1 atm argon gas, and the tube was flame sealed or sealed with epoxy glue. The samples of **2a**, **2b**, and **2c** were placed in a stream of dry nitrogen gas at low temperature (211−225 K). The crystal temperature was maintained by the use of a Rigaku liquid nitrogen cryostat. All measurements were made on a Rigaku AFC7R diffractometer with graphite monochromated Mo Kα (λ = 0.71069 Å) radiation and a 12 kW rotating anode generator. The intensity data were measured using the $\omega-2\theta$ scan technique. The weak reflections ($I < 10.0\sigma(I)$) were rescaned (maximum of five scans), and the counts were accumulated to ensure good counting statistics. Stationary background counts were recorded on each side of the reflection. The ratio of peak counting time to background counting time was 2:1. The intensities of three representative reflection were measured after every 150 reflections and showed no statistically significant change during data collection. Intensity data corrections were made for Lorentz-polarization factors for all data. The structures were solved by direct methods using SHELXS86 programs and expanded using Fourier techniques[3,4] which revealed the positions of all non-hydrogen atoms in the compounds.

Refinement of 2a. The structure was refined upon *F* (full-matrix least-squares method). In the final cycle of the refinement, all hydrogen atoms could be located in the difference density maps. The non-hydrogen and hydrogen atoms were refined on reasonable positions.

Refinement of 2b. The structure was refined upon *F* (full-matrix least-squares method). All non-hydrogen atoms were refined with anisotropic temperature factors. The further cycles of refinement revealed the positional parameters of the hydrogen atoms. The isotropic temperature factors of the hydrogen atoms were constrained to be $U_{iso}(H) = 1.10U_{eq}(C)$ of the corresponding carbon atom. The positional parameters and anisotropic displacement parameters of the non-hydrogen atoms were refined. The hydrogen atoms were included in the

(3) Sheldrick, G. M. SHELXS86. Program for the Solution of Crystal Structure. Univ. of Goettingen, Germany (1985).

(4) Beurskens, P. T.; Admiraal, G.; Beurskens, G.; Bosman, W. P.; Garcia-Granda, S.; Gould, R. O.; Smits, J. M. M.; Smykalla, C.; DIRDIF92. The DIRDIF program system, Technical Report of the Crystallography Laboratory, University of Nijmegen, The Netherlands (1992).

Table 1. Crystallographic Data for the Dewar Pyrimidinones 2a, 2b, and 2c

	2a	2b	2c
formula	$C_{10}H_{16}N_2O$	$C_{16}H_{20}N_2O$	$C_{17}H_{22}N_2O$
fw, g mol^{-1}	180.25	256.35	270.37
crystal system	monoclinic	monoclinic	orthorhombic
space group	$P2_1/c$	$P2_1/c$	*Pbca*
a (Å)	10.026(5)	9.520(3)	17.421(9)
b (Å)	8.96(1)	16.345(3)	17.07(2)
c (Å)	11.969(6)	10.661(2)	10.785(9)
β (deg)	94.73(4)	115.74(1)	90
V (Å^3)	1071(1)	1494.3(6)	3207(7)
Z	4	4	8
crystal size, mm	0.12 × 0.38 × 0.48	0.27 × 0.40 × 0.46	0.14 × 0.20 × 0.43
F_{000}	392.0	552.0	1168.0
D(calc) (g cm^{-3})	1.117	1.139	1.120
μ(Mo Kα) (cm^{-1})	0.73	0.72	0.70
T(K)	211(3)	221(3)	225(3)
2θ scan range (deg)	3.41− 55.0	4.25− 55.0	3.34−50.0
h min, *h* max	0, 13	0, 12	0, 20
k min, *k* max	0, 11	0, 21	0, 20
l min, *l* max	−15, 15	−13, 12	−12, 0
measured reflections	3058	3757	3209
independent reflections	2633	3554	3209
observed reflections [a]	1429	2320	1187
total variables	183	173	270
R[b]	0.041	0.050	0.042
R_w[c]	0.056	0.075	0.054
goodness of fit	1.19	1.76	1.15
secondary extinction	1.300 × 10^{-6}	1.725 × 10^{-6}	5.361 × 10^{-7}
$\Delta\rho_{max}$ and $\Delta\rho_{min}$[d]	0.20 and −0.12	0.26 and −0.24	0.12 and −0.14

[a] $I > 3.00\ \sigma(I)$. [b] $R = \sum||F_o| - |F_c||/\sum|F_o|$. [c] $R_w = \{\sum w(|F_o| - |F_c|)^2/\sum wF_o^2\}^{1/2}$, $w = \{\sigma^2(F_o) + 0.0009F_o^2\}^{-1}$. [d] e Å^{-3}.

refinement but not refined. In the reflection data of **2b**, one reflection (5,1,−3), which was considered to be measured wrong in view of the counting statistics, was deleted.

Refinement of 2c. The structure was refined upon *F* (full-matrix least-squares method). In the final cycle of the refinement, all hydrogen atoms could be located in the difference density maps. The non-hydrogen and hydrogen atoms were refined on reasonable positions.

Neutral atom scattering factors were taken from Cromer and Waber.[5] Anomalous dispersion effects were included in F_{calc};[6] the values for $\Delta f'$ and $\Delta f''$ were those of Creagh and McAuley.[7] The values for the mass attenuation coefficients were those of Creagh and Hubbell.[8] All calculations were performed using the teXsan[9] crystallographic software package of Molecular Structure Corporation.

Theoretical Calculations

Ab initio LCAO-MO methods[10] were used in the calculation of **2a**, 1,3,6-trimethyl-5-oxo-2,6-diazabicyclo[2.2.0]hex-2-ene (**2d**), 1,6-dimethyl-5-oxo-2,6-diazabicyclo[2.2.0]hex-2-ene (**2e**), 3,6-dimethyl-5-oxo-2,6-diazabicyclo[2.2.0]hex-2-ene (**2f**), 6-methyl-5-oxo-2,6-diazabicyclo[2.2.0]hex-2-ene (**2g**) and 5-oxo-2,6-diazabicyclo[2.2.0]hex-2-ene (**2h**), 2-azetidinone (**9**), 3,4-dihydroazete (**11**), and (*E*)- and (*Z*)-*N*-ethylidenemethylamines (**12**). All calculations were carried out using Gaussian 92 and Gaussian 94 suites of programs.[11] The geometries for the molecules were fully optimized at HF/6-31G(d, p) and MP2/6-31G(d, p) utilizing analytical gradient techniques and default threshold for convergence. The "frozen core approximation" was used; 1s electrons of C, N, and O atoms were not included in an electron correlation energy calculation. The calculations of the Dewar isomers **2d**−**h**, and **9**, **11**, **12** were undertaken on a Gateway 2000 (P5-90) microcomputer. The HF and MP2 level calculations of 3-*tert*-butyl-1,6-dimethyl Dewar pyrimidinone **2a** were performed on a CrayYMP-Unicos.

Results and Discussion

Crystal Structure. The structures of the Dewar pyrimidinones **2a**−**h** are illustrated in Figure 2 and the atom numbering scheme of the functional groups are shown in Figures 2−5. The structures of the Dewar pyrimidinones **2a**−**c** were determined by single-crystal X-ray diffraction studies. The X-ray data of **2a**−**c** were measured at room temperature (294−296 K) and low temperature (211−225 K). The data obtained at room temperature led to the similar results derived from those at low temperature. However, the crystal structural data at room temperature are less precise and reliable because of the weak diffracting power caused by intense thermal motions of the methyl and phenyl groups. Then, only the low temperature measurements and results are discussed here in detail.

The crystallographic data for **2a**−**c** are summarized in Table 1. The selected bond distances, bond angles, and dihedral angles of **2a**−**c** are shown in Table 2. The ORTEP diagrams of the Dewar pyrimidinones **2a**, **2b**, and **2c** are presented in Figures 3−5, respectively. Table

(5) Cromer, D. T.; Waber, J. T. *International Tables for X-ray Crystallography*; Kynoch Press: Birmingham, England, 1974; Vol. 4, pp 71−98.

(6) Ibers, J. A.; Hamilton, W. C. *Acta Crystallogr.* **1964**, *17*, 781−782.

(7) Creagh, D. C.; McAuley, W. J. *International Tables for Crystallography*; Kluwer Academic Publishers: Boston, 1992; Vol. C, Table 4.2.6.8, pp 219−222

(8) Creagh, D. C.; Hubbell, J. H. *International Tables for Crystallography*; Kluwer Academic Publishers: Boston, 1992; Vol. C, Table 4.2.4.3, pp 200−206.

(9) Crystal Structure Analysis Package, Molecular Structure Corporation: The Woodlands, TX, 1985 and 1992.

(10) Hehre, W. J.; Radom, L.; Schleyer, P.v.R.; Pople, J. A. *Ab Initio Molecular Orbital Theory*; Wiley: New York, 1986.

(11) (a) Gaussian 92, 486-Windows-G92 Revision E.1 and Gaussian 92, CrayYMP-Unicos-G92 Revision G.1. Frisch, M. J.; Trucks, G. W.; Head-Gordon, M.; Gill, P. M.W.; Wong, M. W.; Foresman, J. B.; Johnson, B. G.; Schlegel, H. B.; Robb, M. A.; Replogle, E. S.; Gomperts, R.; Andres, J. L.; Raghavachari, K.; Binkley, J. S.; Gonzalez, C.; Martin, R. L.; Fox, D. J.; DeFrees, D. J.; Baker, J.; Stewart, J. P.; Pople, J. A., Gaussian, Inc., Pittsburgh, PA, 1992. (b) Gaussian 94, Revision B.2, Frisch, M. J.; Trucks, G. W.; Schlegel, H. B.; Gill, P. M. W.; Johnson, B. G.; Robb, M. A.; Cheeseman, J. R.; Keith, T.; Petersson, G.A.; Montgomery, J. A.; Raghavachari, K.; Al-Laham, M. A.; Zakrzewski, V. G.; Ortiz, J. V.; Foresman, J. B.; Peng, C. Y.; Ayala, P. Y.; Chen, W.; Wong, M. W.; Andres, J. L.; Replogle, E. S.; Gomperts, R.; Martin, R. L.; Fox, D. J.; Binkley, J. S.; Defrees, D. J.; Baker, J.; Stewart, J. P.; Head-Gordon, M.; Gonzalez, C.; Pople, J. A.; Gaussian, Inc., Pittsburgh, PA, 1995.

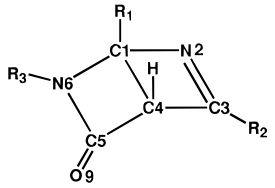

compound	R_1[a,b]	R_2[a,c]	R_3[d]
2a	CH_3	t-Bu	CH_3
2b	$C_6H_5CH_2$	t-Bu	CH_3
2c	p-$CH_3C_6H_4CH_2$	t-Bu	CH_3
2d	CH_3	CH_3	CH_3
2e	CH_3	H	CH_3
2f	H	CH_3	CH_3
2g	H	H	CH_3
2h	H	H	H

a) The atomic numbering of the tert-butyl, benzyl, and p-methylbenzyl group of the Dewar isomers (**2a**, **2b**, and **2c**) is shown in Fig. **3-5**.

b) R_1: H1, H7'–C7(H7)–H7''

c) R_2: H3, H8'–C8(H8)–H8''

d) R_3: H6, H10'–C10(H10)–H10''

Figure 2. The structures of the Dewar pyrimidinones **2a**−**h** and the atom numbering scheme used for the functional groups.

Table 2. Selected Bond Distances (Å), Bond Angles (deg), and Dihedral Angles (deg) of the Dewar Pyrimidinones 2a−c Obtained by X-ray Diffraction Analysis

bond and angles	**2a**	**2b**	**2c**
C1−N2	1.520(2)	1.523(2)	1.517(4)
C1−C4	1.549(3)	1.553(2)	1.549(5)
C1−N6	1.461(2)	1.456(2)	1.456(4)
C1−C7	1.494(3)	1.497(3)	1.496(5)
N2−C3	1.286(3)	1.292(2)	1.286(4)
C3−C4	1.520(3)	1.521(3)	1.516(5)
C3−C8	1.495(3)	1.492(3)	1.502(5)
C4−C5	1.535(3)	1.535(3)	1.544(6)
C5−N6	1.361(3)	1.359(3)	1.352(5)
C5−O9	1.211(2)	1.214(2)	1.210(5)
N6−C10	1.450(3)	1.448(3)	1.451(5)
C8−C11	1.532(3)	1.505(3)	1.534(6)
C8−C12	1.520(3)	1.517(3)	1.509(6)
C8−C13	1.531(3)	1.531(3)	1.525(6)
C1−N2−C3	90.1(1)	90.3(1)	90.1(3)
C1−C4−C3	81.0(1)	81.3(1)	81.0(3)
C1−C4−C5	84.7(2)	84.4(1)	84.0(3)
C1−N6−C5	94.7(2)	94.9(1)	94.9(3)
C1−N6−C10	129.9(2)	129.7(2)	130.4(4)
N2−C1−C4	89.0(1)	88.8(1)	89.0(3)
N2−C1−N6	112.0(2)	112.6(1)	113.1(3)
N2−C1−C7	115.8(2)	113.5(1)	113.2(3)
N2−C3−C4	99.8(2)	99.5(2)	99.8(3)
N2−C3−C8	129.9(2)	128.5(2)	129.1(3)
C3−C4−C5	110.8(2)	111.1(1)	111.7(3)
C3−C8−C11	107.7(2)	108.5(2)	107.1(3)
C3−C8−C12	110.5(2)	109.6(2)	109.4(3)
C3−C8−C13	107.9(2)	107.6(2)	108.4(3)
C4−C1−N6	88.1(1)	88.1(1)	88.4(3)
C4−C1−C7	127.6(2)	129.0(2)	128.9(3)
C4−C3−C8	130.3(2)	132.0(2)	131.0(3)
C4−C5−N6	92.4(2)	92.4(1)	92.5(3)
C4−C5−O9	135.8(2)	135.8(2)	134.8(4)
C5−N6−C10	130.0(2)	130.0(2)	130.5(4)
N6−C1−C7	118.7(2)	119.7(2)	119.3(3)
N6−C5−O9	131.8(2)	131.8(2)	132.7(4)
N2−C1−C4−C5	−109.8(1)	−109.5(1)	−110.0(3)
N6−C1−C4−C3	114.4(1)	115.4(1)	116.2(3)

1S (Supporting Information) shows the results of the least-squares planes for **2a**−**c**. Excellent agreement among three Dewar pyrimidinones **2a**−**c** was found in the bond distances, angles, and dihedral angles. The respective differences in the bond distances, bond angles, and dihedral angles are 0.002 Å, 0.3°, and 0.4° on the average, which are in the range of the standard deviations. Then, the average bond distances and angles of the Dewar pyrimidinones **2a**, **2b**, and **2c** are used for comparison with those of the related compounds. The three alkyl substituents (methyl, benzyl, and *p*-methylbenzyl groups) at the C1 position do not virtually affect the geometry of the Dewar pyrimidinone moieties. The bond angles in the 2-azetidinone and dihydroazete moieties are nearly 90° (81−100°). This suggests that the Dewar pyrimidinone is an extremely strained molecule. The both dihydroazete and 2-azetidinone rings are nearly planar with mean deviations of 0.016−0.022 Å from the least-squares plane. The angles between the least-squares planes of the dihydroazete and 2-azetidinone rings are 112−113°, which is close to the tetrahedral angle (109.5°). The sums of the angles at the amide N atom are 354.6° in **2a**, 354.5° in **2b**, and 355.6° in **2c**. The configuration at the amide N6 atom is nearly planar, suggesting a significant sp^2 character for the N6 atom.

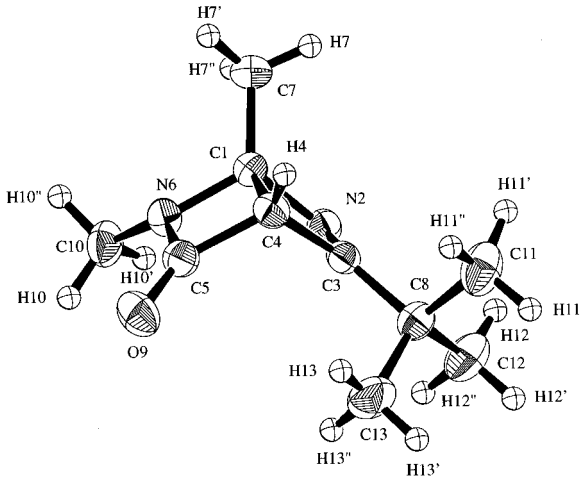

Figure 3. The X-ray structure and the numbering scheme for the Dewar pyrimidinone **2a**. The thermal ellipsoid is drawn at the 50% probability level.

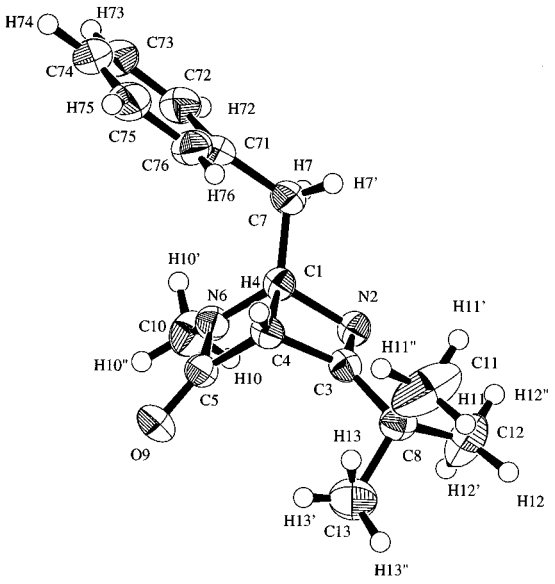

Figure 4. The X-ray structure and the numbering scheme for the Dewar pyrimidinone **2b**. The thermal ellipsoid is drawn at the 50% probability level.

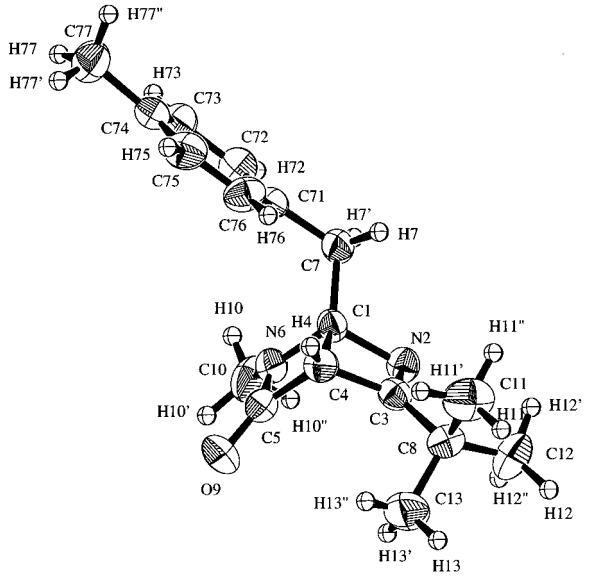

Figure 5. The X-ray structure and the numbering scheme for the Dewar pyrimidinone **2c**. The thermal ellipsoid is drawn at the 50% probability level.

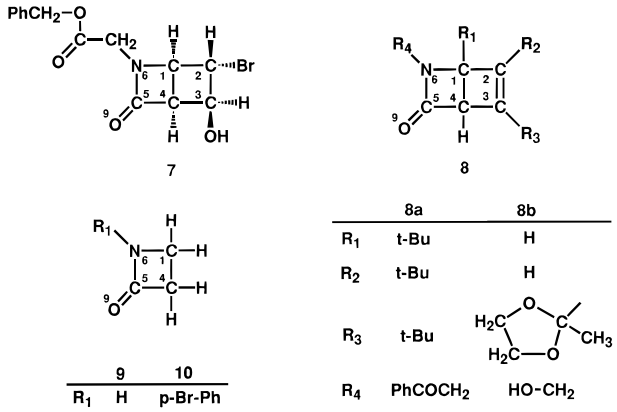

Figure 6. The structures of the Dewar pyridones **7** and **8** and 2-azetidinones **9** and **10**. The numbering scheme corresponds to that of the Dewar pyrimidinone **2**. The nonstandard atom numbering scheme of the compounds was used so as to aid comparison of the corresponding bond distances and bond angles.

In the Dewar isomers **2b** and **2c**, the benzene ring is directed toward the plane of the 2-azetidinone ring (see Figures 4 and 5). This may be due to steric repulsion between the phenyl and *tert*-butyl groups.

The bond distances and angles of the 2-azetidinone ring in the Dewar pyrimidinone **2** are compared with those of the Dewar pyridone derivatives (**7**, **8a,** and **8b**)[12] and monocyclic 2-azetidinones (**9** and **10**).[13] The structures and numbering schemes are illustrated in Figure 6. The selected bond distances and angles are shown in Table 3. The C1−C4, C1−N6, C4−C5, C5−N6, and C5−O9 bond distances of the Dewar pyrimidinones **2a**−**c** are almost the same as those of the typical values[14,15] and

Table 3. Selected Bond Distances (Å) and Angles (deg) of the Dewar Pyrimidinone 2,[a] Dewar Pyridones 7,[12a] 8a,[12b] and 8b,[12c] and 2-Azetidinones 9[13a] and 10[13b] Obtained by X-ray Diffraction Analysis

geometry	2[a]	7	8a	8b	9	10
C1−C4	1.550	1.551(11)	1.541(8)	1.619(6)	1.538(2)	1.539(7)
C1−N6	1.458	1.471(9)	1.494(6)	1.474(6)	1.467(2)	1.459(7)
C4−C5	1.538	1.529(11)	1.501(9)	1.536(6)	1.522(2)	1.518(7)
C5−N6	1.357	1.344(10)	1.359(7)	1.379(5)	1.333(2)	1.363(7)
C5−O9	1.212	1.220(10)	1.206(7)	1.242(5)	1.226(1)	1.207(7)
C1−C4−C5	84.4	85.4(6)	87.6(4)	84.6(2)	85.9(1)	85.4(3)
C1−N6−C5	94.8	95.8(6)	95.1(4)	96.1(3)	96.2(1)	94.5(3)
C4−C1−N6	88.2	86.6(6)	85.4(4)	86.1(2)	86.2(1)	87.9(3)
C4−C5−N6	92.4	92.1(7)	91.9(5)	92.9(3)	91.7(1)	92.0(3)
C4−C5−O9	135.5	135.0(8)	137.8(6)	135.4(3)	135.9(1)	136.5(3)
N6−C5−O9	132.1	132.8(8)	130.2(6)	131.7(3)	132.4(1)	131.1(3)

[a] Average values of the present X-ray diffraction data of the Dewar pyrimidinones **2a**−**c**.

are similar to the corresponding ones of the Dewar pyridone derivative **7**, 2-azetidinone (**9**), and 1-(4-bromophenyl)-2-azetidinone (**10**). The variations in the bond distances of the 2-azetidinone ring of the compounds (**2**, **7**, **9**, and **10**) are as small as 0.005 Å to as large as 0.024 Å and ca. 0.010 Å on the average, indicating little or no structural change of the 2-azetidinone ring by fusion with the dihydroazete or cyclobutane rings. The bond distances and angles of the 2-azetidinone moiety in the Dewar pyridones **8** vary remarkably by substituent groups. The bond distances of the C1−N6 in **8a** and of the C1−C4 and C5−O9 in **8b** are significantly lengthened from the typical bond distances[14,15] (differences 0.030, 0.071, and 0.044 Å, respectively). The C4−C5 bond distance in **8a** is shortened by ca. 0.03 Å than the typical values.[14,15] Therefore, we cannot find systematic structural changes in the azetidinone ring by fusion with the cyclobutene ring.

No experimental structural data on the dihydroazete and its derivatives was available in the literature. The bond distances of the N2=C3 (1.288 Å) and C3−C4 (1.518 Å) of **2a**−**c** are close to the typical values {reference value[14] for a Car-N=CH−C bond [1.279(8) Å] and that for a C*−C=C (endocyclic) in cyclobutane [1.513(18) Å], respectively}. The C1−N2 bond distance (1.520 Å) is lengthened by 0.055 Å when compared with the typical straight-chain single C−N(=C) bond distance [reference[14] value for a (C*)−N(=CH−Car) bond, 1.465(11) Å]. The abnormal C1−N2 elongation that is inferred from the reactivities of the Dewar molecules is due to ring strain of the four-membered cyclic imine moiety. The C3−C8 (1.496 Å) and N6−C10 (1.450 Å) bond distances are close to the respective typical values {reference[14] value for a C*−C=C (exocyclic) in cyclobutenyl-C* [1.489(15) Å] and that for a C*−N(−C*)−C=O (exo) in γ-lactams [1.458-(14) Å)]}. The C1−C7 bond distance (1.496 Å) is significantly shortened by 0.033 Å from that of a typical Csp^3−Csp^3 bond [reference[14] value for a cyclobutyl−C* (exocyclic), 1.529(16) Å] and is close to an sp^2-hybridized bond distance [reference[14] value for a C*−C=C (exocyclic) in cyclobutenyl−C*, 1.489(15) Å].

(12) (a) *N*-[(Benzyloxycarbonyl)methyl]-6-bromo-5-hydroxy-3-oxo-2-azabicyclo[2.2.0]hexane (**7**): Begley, W. J.; Lowe, G.; Cheetham, A. K.; Newsam, J. M. *J. Chem. Soc., Perkin Trans. 1* **1981**, 2620−2624. (b) 2-(Benzoylmethyl)-1,5,6-tri-*tert*-butyl-2-azabicyclo[2.2.0]hex-5-en-3-one (**8a**): Regitz, M.; Michels, G. *Chem. Ber.* **1990**, *123*, 927−933. (c) (−)-(1*S*,4*R*)-*N*-(hydroxymethyl)-5-(2-methyl-1,3-dioxolan-2-yl)-2-azabicyclo[2.2.0]hex-5-en-3-one (**8b**)**:** Nakano, H.; Iwasa, K.; Kabuto, C.; Matsuzaki, H.; Hongo, H. *Chem. Pharm. Bull.* **1995**, *43*, 1254−1256.

(13) (a) **9**: Yang, Q.-C.; Seiler, P.; Dunitz, J. D. *Acta Crystallogr.* **1987**, *C43*, 565−567. (b) 1-(4-Bromophenyl)-2-azetidinone (**10**): Kartha, G.; Ambady, G. *J. Chem. Soc., Perkin Trans. 2* **1973**, 2042−2044.

(14) Allen, F. H.; Kennard, O.; Watson, D. G.; Brammer, L.; Orpen, A. G.; Taylor, R. In *International Tables for Crystallography*; Wilson, A. J. C., Ed.; Kluwer Academic Publishers: Dordrecht, 1992; Volume C, pp 685−706.

(15) The typical bond distances of the C1−C4, C1−N6, C4−C5, C5−N6, and C5−O9 in the 2-azetidinone ring are the following values: C1−C4 {reference[14] value for a C*−C* in azetine [1.548(18) Å]}; C1−N6 {that for a β-lactam C*−N(X)−C=O (endo) [1.464(12) Å]}; C4−C5 {that for a $(C^*)_2$−C=O in cyclobutanone [1.529(16) Å]}; C5−N6 [that for a C*−NH−C=O in β-lactams, 1.385(19) Å]; C5−O9 {that for a C*−NH−C=O in β-lactams [1.198(12) Å]}.

Table 4. Optimized Geometries of the Dewar Pyrimidinones 2a,d−h Calculated at the MP2/6-31G(d,p) Levels. Selected Geometrical Parameters are given in Angstroms for Bond Distances and Degrees for Bond Angles

geometry	2a	2d	2e	2f	2g	2h
C1−N2	1.517	1.519	1.524	1.512	1.517	1.515
C1−C4	1.550	1.550	1.553	1.543	1.547	1.548
C1−N6	1.462	1.461	1.458	1.454	1.451	1.452
C1−C7	1.498	1.498	1.498			
N2−C3	1.309	1.307	1.304	1.308	1.304	1.304
C3−C4	1.520	1.515	1.508	1.517	1.509	1.507
C3−C8	1.493	1.485		1.485		
C4−C5	1.542	1.544	1.547	1.546	1.549	1.551
C5−N6	1.387	1.387	1.387	1.388	1.388	1.393
C5−O9	1.219	1.218	1.217	1.217	1.216	1.213
N6−C10	1.447	1.447	1.447	1.447	1.447	
C1−N2−C3	88.95	88.99	88.53	88.88	88.45	88.60
C1−C4−C3	80.59	80.77	80.58	80.61	80.45	80.49
C1−C4−C5	84.90	84.84	84.69	84.62	84.48	84.66
C1−N6−C5	94.13	94.22	94.44	94.02	94.25	94.36
N2−C1−C4	90.21	89.95	89.80	90.39	90.22	90.11
N2−C1−N6	112.67	112.71	112.77	114.21	114.25	114.97
N2−C3−C4	100.11	100.14	100.92	100.02	100.77	100.68
C3−C4−C5	109.67	109.77	110.16	110.12	110.48	110.78
C4−C1−N6	88.74	88.80	88.83	89.27	89.30	89.19
C4−C5−N6	91.87	91.77	91.72	91.61	91.55	91.27
C4−C5−O9	135.88	136.00	136.05	136.10	136.14	135.64
N6−C5−O9	132.19	132.18	132.21	132.25	132.29	133.10

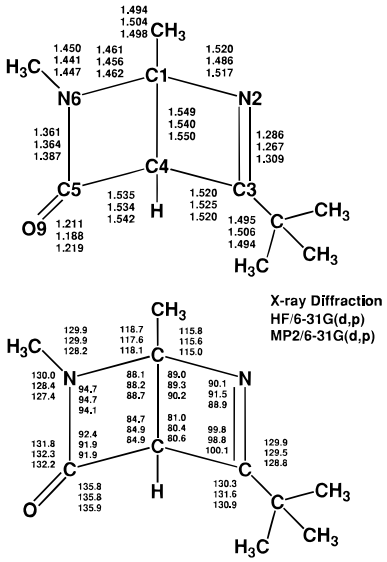

Figure 7. Bond distances (Å) and bond angles (deg) of X-ray diffraction, HF/6-31G(d,p), and MP2/6-31G(d,p) for **2a**.

Comparison between ab Initio and X-ray Diffraction Structures of 2a. The bond distances and bond angles of the MP2/6-31G(d,p) and HF/6-31G(d,p) optimizations of the Dewar isomer **2a** are illustrated in Figure 7 and are compared with the X-ray diffraction data. Most of differences in the bond distances between the ab initio calculations and experiment are within 0.010 Å on the average and are as small as 0.001 Å to as large as 0.034 Å. The differences of the bond angles are approximately 0.7° on the average. The deviations of the HF and MP2 bond distances from the experimental values are 0.012 Å and 0.008 Å on the average, respectively. The HF C1−N2 bond distance is close to a typical straight-chain bond distance, and the MP2 C1−N2 bond distance is the same as the experimental C1−N2 value within the error limits of the structure determinations. The results indicate the importance of full geometry optimization by incorporation of electron correlation in the wave function. The remarkable deviations between the HF calculations and experimental values are found at the C1−N2, N2═C3, and C5═O9 bonds. These bond distances deviate from 0.019 to 0.034 Å. The differences in the bond distances of the C1−N2 and C5═O9 bond decrease markedly after inclusion of electron correlation effects. The deviations (0.023 Å and 0.026 Å) in the N2═C3 and C5−N6 bond distances between the MP2 calculation and experimental data may be due to neglect of higher order electron correlations such as MP3 and MP4 calculations. However, the most of the bond distances and angles of **2a** are in good agreement between the MP2 calculation and experimental data.

Optimized Structures of the Dewar Pyrimidinones 2a,d−h. As described above, the products of the 1,3,6-trialkyl Dewar pyrimidinones **2a** and **2d** in methanol are the 4-methoxy-2-azetidinones **3**.[1a,f] However, irradiation of the 2,3-dimethyl-, 3,6-dimethyl-, 3-methyl-, and nonsubstituted 4(3*H*)-pyrimidinones **1** does not give the expected product. We have considered the drastic substituent effects by alkyl groups may be due to variation of the C1−N2 bond distance in the Dewar isomers **2** or to increase in stability of the intermediates. The examination of the latter suggestion is difficult at the present time because the calculations on transition states of the larger molecules need an enormous amount of CPU time and other resources. The former suggestion can be readily examined by the ab initio calculations of the alkyl-substituted Dewar isomers **2**. We have undertaken ab initio calculations of the substituted Dewar pyrimidinones **2d**−**h** at the HF/6-31G(d,p) and MP2/6-31G(d,p) levels of theory in order to better understand the substituent effects. The results of the MP2/6-31G(d,p) level calculation are used for comparison of the bond distances and angles of the substituted Dewars **2**. The selected MP2 bond distances and angles of the Dewar pyrimidinones **2a** and **2d**−**h** are summarized in Table 4. The bond distances and angles of the alkyl substituted Dewar pyrimidinones (**2a** and **2d**−**g**) are compared with those of the nonsubstituted Dewar isomer **2h**. The C4−C5 and C5−N6 bond distances of the Dewars **2a** and **2d**−**g** are shorter by ca. 0.005 Å on the average, and the C5−O9 bond distance is longer by ca. 0.005 Å on the average than those of **2h**. The both C4−C5−O9 and C4−C5−N6 bond angles of the Dewars **2a** and **2d**−**g** are larger by ca. 0.4° on the average, and the N6−C5−O9 bond angle is smaller by ca. 0.9° on the average than those of **2h**. The variations of the bond distances and angles between the

Dewars **2a** and **2d**−**g** and **2h** are apparently due to change of the conjugated system at the N6, C5, and O9 atoms by the substitution of the hydrogen for the methyl group at the 6 position, because the variations are approximately constant and independent of the positions of the alkyl groups. The N2−C1−N6 and C3−C4−C5 bond angles of the Dewars **2a** and **2d**−**g** are smaller than those of **2h**. The differences are 0.7−2.3° and 0.3−1.1°, respectively. The differences of the bond angles depend on the position of the alkyl groups and may be responsible for steric repulsion between the alkyl groups and the atoms in the rings (N2, C3, C5, and N6 atoms) except for the bridgehead C1 and C4 atoms. These steric effects are limited to only the N2, C3, C5, and N6 atoms, and the geometries of the Dewar pyrimidinones **2a** and **2d**−**g** are almost identical with that of the Dewar **2h**.

Further geometry optimization of the Dewar isomer **2h** at the HF/6-311G(d,p) level of theory was undertaken with expectation that the HF calculation might give a result similar to that of MP2 calculation when a larger basis set is used. The obtained geometrical data were virtually the same as those obtained with the 6-31G(d,p) basis set. The analogous results on the Dewar isomer **2g** have been reported.[2c] The larger basis set at HF level calculation does not give improved geometrical structures. This verifies that the geometry optimizations at the MP2 level of theory are important for the Dewar compounds for calculating structures. Furthermore, in order to test whether the theoretically calculated geometry is sufficiently converged at the MP2/6-31G(d,p) level of theory, full geometrical optimizations of the Dewar isomer **2h** have been carried out at the MP2(full)/6-31G(d,p), MP2/6-311G(2d,p), and MP2/6-31+G(d,p) levels of theory. The results were quite similar to that of the MP2/6-31G(d,p). The differences in the bond distances are from ca. 0.002 to 0.004 Å. The 6-31G(d,p) basis set is sufficient at the MP2 level of theory.

Natural Bond Orbital Analysis of the Dewar Pyrimidinones 2d−**h**. The natural bond orbital (NBO) analysis[16] of the Dewars **2d**−**h** has been carried out to examine the change of the bond character on the orbital hybridization by substitution of the alkyl groups. It is convenient to define the hybridization factor *n* in terms of p character index (sp^n). The results are summarized in Table 5. The significant variations of the hybridization characters are not observed, indicating the minor substitution effect on the orbital hybridization by the alkyl groups. The results may indicate that the drastic substituent effects in the reactions of the Dewar isomers are related to thermodynamic stability of intermediates. The N6 atom and its lone pair have the sp^2 hybridization and pure p characters, respectively. The bridgehead C1 and C4 atoms are $sp^{2.26-1.99}$ hybridization character in the C1−C7, C1−H1, and C4−H4 bonds. The X-ray planar configuration of the N6 atom and shorter X-ray C1−C7 bond distance than a typical Csp^3−Csp^3 bond distance are consistent with the sp^2 character of the N6 and C1 atoms.

Optimized Geometries of the Compounds 2h, 9, 11, and (*E*)- and (*Z*)-12. The ab initio calculations of 2-azetidinone (**9**), dihydroazete **11**, and (*E*)- and (*Z*)-*N*-ethylidenemethylamines (**12**) have been carried out to compare the structures of the 2-azetidinone and dihydroazete rings in the Dewar pyrimidinone **2h** with the structures of the compounds **9**, **11**, and **12**. The compounds **9**, **11**, and (*E*)-**12** were prepared,[17] and their NMR,[18] IR,[19] photoelectron spectra (PE),[20] and microwave spectra[21] were reported. The structure of **9** was experimentally determined by X-ray diffraction analysis[13a] in crystal and by electron diffraction analysis[21a] in gas phase. However, no experimental structural determination of **11** and (*E*)-**12** has been published. The semiempirical and ab initio computations of the 2-azetidinone **9**,[21a,22−25] dihydroazete **11**,[20,21b,26] and (*E*)- and (*Z*)-imines **12**[20,27] were reported. In the present study, full geometry optimizations of the compounds **9**, **11**, and **12** have been

Table 5. Natural Bond Orbital Hybridization Analysis of the Dewar Pyrimidinones 2d−h at MP2/6-31G(d,p) Level Calculations

		hybridization sp^n				
bond	atom	**2d** *n*	**2e** *n*	**2f** *n*	**2g** *n*	**2h** *n*
C1−N2	C1	3.67	3.74	3.41	3.47	3.42
	N2	3.25	3.25	3.43	3.44	3.43
C1−C4	C1	3.27	3.29	3.22	3.23	3.23
	C4	3.82	3.84	3.97	3.99	3.98
C1−N6	C1	3.55	3.51	3.36	3.32	3.37
	N6	2.31	2.30	2.40	2.39	2.22
C1−C7	C1	2.00	1.99			
	C7	2.50	2.51			
N2−C3	N2	1.70	1.79	1.68	1.76	1.77
	C3	2.16	2.11	2.17	2.12	2.12
C3−C4	C3	2.14	1.99	2.16	2.00	2.00
	C4	3.07	3.12	3.03	3.08	3.06
C3−C8	C3	1.74		1.72		
	C8	2.59		2.60		
C4−C5	C4	3.23	3.19	3.20	3.16	3.19
	C5	1.97	1.98	1.98	1.99	1.98
C5−N6	C5	2.19	2.19	2.19	2.19	2.22
	N6	2.25	2.24	2.22	2.21	2.10
C5−O9	C5	1.94	1.95	1.93	1.93	1.89
	O9	1.36	1.37	1.36	1.37	1.34
N6−C10	N6	1.95	1.94	1.91	1.89	
	C10	3.31	3.32	3.31	3.33	
LP N2[a]	N2	1.52	1.45	1.48	1.41	1.41
LP N6[a]	N6	18.32	19.83	18.31	20.01	15.23
LP O9[a]	O9	0.76	0.76	0.76	0.76	0.77
C1−H1	C1			2.26	2.24	2.24
C3−H3	C3		1.91		1.89	1.89
C4−H4	C4	2.24	2.22	2.22	2.19	2.19
N6−H6	N6					2.28
C7−H7	C7	3.19	3.17			
C7−H7′	C7	3.21	3.21			
C7−H7″	C7	3.17	3.18			
C8−H8	C8	3.19		3.19		
C8−H8′	C8	3.21		3.21		
C8−H8″	C8	3.04		3.04		
C10−H10	C10	2.92	2.92	2.92	2.92	
C10−H10′	C10	2.87	2.87	2.87	2.87	
C10−H10″	C10	2.88	2.88	2.88	2.87	

[a] LP stands for lone pair.

(16) (a) Foster, J. P.; Weinhold, F. *J. Am. Chem. Soc.* **1980**, *102*, 7211−7218. (b) NBO Version 3.1, Glendening, E. D.; Reed, A. E.; Carpenter, J. E.; Weinhold, F.

(17) (a) **9**: Pfaendler, H. R.; Hoppe, H. *Heterocycles* **1985**, *23*, 265−272. (b) **11**: Guillemin, J. C.; Denis, J. M.; Lablache-Combier, A. *J. Am. Chem. Soc.* **1981**, *103*, 468−469. (c) (*E*)-**12**: Meier, J.; Akermann, F.; Guenthard, Hs. H. *Helv. Chim. Acta* **1968**, *51*, 1686−1691.

(18) (a) **9**: reference 17a; **11**: reference 17b; (*E*)-**12**: reference 17c.

(19) (a) **9**: Hanai, K.; Maki, Y.; Kuwae, A. *Bull. Chem. Soc. Jpn.* **1985**, *58*, 1367−1375. (b) **11**: Amatsu, Y.; Hamada, Y.; Tsuboi, M. *J. Mol. Spectrosc.* **1987**, *123*, 267−275. (c) (*E*)-**12**: reference 17c.

(20) **11** and (*E*)-**12**: Bock, H.; Dammel, R. *Chem. Ber.* **1987**, *120*, 1971−1985.

(21) (a) **9**: Marstokk, K.-M.; Moellendal, H.; Samdal, S.; Uggerud, E. *Acta Chem. Scand.* **1989**, *43*, 351−363. (b) **11**: Sugie, M.; Takeo, H.; Matsumura, C. *J. Am. Chem. Soc.* **1989**, *111*, 906−910. (c) (*E*)-**12**: Meier, J.; Bauder, A.; Guenthard, Hs. H. *J. Chem. Phys.* **1972**, *57*, 1219−1236.

(22) Treschanke, L.; Rademacher, P. *J. Mol. Struct. (THEOCHEM)* **1985**, *122*, 35−45.

(23) Cossio, F. P.; Ugalde, J. M.; Lopez, X.; Lecea, B.; Palomo, C. *J. Am. Chem. Soc.* **1993**, *115*, 995−1004.

(24) Sedano, E.; Ugalde, J. M.; Cossio, F. P.; Palomo, C. *J. Mol. Struct. (THEOCHEM)* **1988**, *166*, 481−486.

Table 6. HF/6-31G(d,p), MP2/6-31G(d,p), and Microwave Rotational Constants[21a−c] of the 2-Azetidinone 9, Dihydroazete 11, and (*E*)-Imine 12

compd	rotational constant[a]	RHF/ 6-31G(d,p)	MP2/ 6-31G(d,p)	microwave
9	A	12442.6589	12296.0349	12161.348(12)
	B	5098.9161	4956.7326	5003.341(11)
	C	3788.2616	3698.1330	3715.787(11)
11	A	14239.3567	14045.0746	13911.630(24)
	B	12963.9498	12694.9389	12713.799(24)
	C	7413.1889	7280.6424	7254.990(24)
(*E*)-**12**	A	39661.1409	38122.0994	38258.627(48)
	B	4104.5204	4093.1894	4078.1354(58)
	C	3896.2026	3872.4963	3862.7391(72)

[a] The calculated and experimental rotational constants are expressed in MHz.

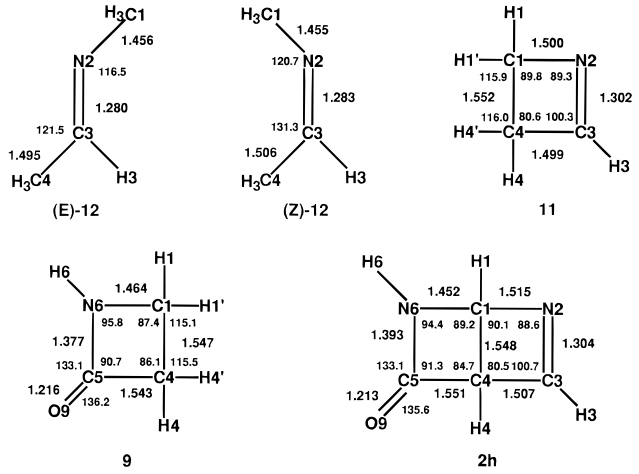

Figure 8. The selected bond distances (Å) and angles (deg) of the Dewar pyrimidinone **2h**, 2-azetidinone **9**, dihydroazete **11**, and (*E*)- and (*Z*)-imines **12**. The numbering scheme corresponds to that of the Dewar pyrimidinone **2h**. The nonstandard atom numbering scheme of the compounds was used so as to aid comparison of the corresponding bond distances and angles at the MP2/6-31G(d,p) level of theory.

undertaken at HF/6-31G(d,p) and MP2/6-31G(d,p) level of theory to obtain the structures of these compounds. Table 6 shows a comparison of the calculated and experimental rotational constants of the 2-azetidinone **9**, dihydroazete **11**, and (*E*)-imine **12** in order to evaluate the quality of HF and MP2 molecular geometries. There is an excellent correspondence between the experimentally derived rotational constants and those calculated at the MP2 level of theory. The selected MP2 bond distances and angles of the compounds **9**, **11**, (*E*)-**12**, and (*Z*)-**12** are listed in Table 2S (Supporting Information), and their selected bond distances and angles are depicted in Figure 8 to compare with those of the Dewar pyrimidinone **2h.** The reported structures of the compounds **9**, **11**, and **12** at HF/6-31G(d), HF/6-31G(d,p), and MP2/6-31G(d,p) are almost the same as the present HF and MP2 structures. The bond distances and angles of the 2-azetidinone ring in the Dewar **2h** are similar to those of **9**, indicating minor structural change of the 2-azetidinone moiety by fusion with the dihydroazete ring. The C1−N2 and N2−C3 bond distances of **2h** are longer by 0.060 Å and 0.021 Å than those of (*Z*)-**12**. Similarly, the C1−N2 and N2−C3 bond distances in the dihydroazete **11** are longer by 0.045 and 0.019 Å than those in (*Z*)-**12**, respectively. The C3−C4 bond distances of the compounds **2h**, **11**, and (*Z*)-**12** are approximately the same. The abnormally long C1−N2 bond distances in **2h** and **11** are related to the reduced C1−N2═C3 and N2═C3−C4 bond angles (89−100°) that are smaller by ca. 31° than those of the straight-chain (*Z*)-imine **12**.

Table 7. NBO Hybridization Analysis of the Dewar Pyrimidinone 2h, 2-Azetidinone 9, Dihydroazete 11, and (*Z*)- and (*E*)-Imines 12 at MP2/6-31G(d,p) Level Calculations

		hybridization sp^n				
bond	atom	**2h** *n*	**9** *n*	**11** *n*	(*Z*)-**12** *n*	(*E*)-**12** *n*
C1−N2	C1	3.42		3.67	3.05	3.03
	N2	3.43		3.28	2.35	2.41
C1−C4	C1	3.23	2.95	2.84		
	C4	3.98	3.10	3.23		
C1−N6	C1	3.37	3.73			
	N6	2.22	2.13			
C1−H	C1	2.24	2.72	2.80	2.81, 3.05	2.89, 3.02
N2−C3	N2	1.77		1.74	1.43	1.46
	C3	2.12		2.13	1.87	1.92
LP N2	N2	1.41		1.47	2.43	2.31
C3−C4	C3	2.00		1.94	1.76	1.91
	C4	3.06		3.15	2.65	2.61
C3−H	C3	1.89		1.93	2.45	2.17
C4−C5	C4	3.19	3.29			
	C5	1.98	1.94			
C4−H	C4	2.19	2.82	2.82	3.20, 2.97	3.20, 3.02
C5−N6	C5	2.22	2.26			
	N6	2.10	1.87			
C5−O9	C5	1.89	1.82			
	O9	1.34	1.31			
N6−H6	N6	2.28	2.02			
LP N6	N6	15.23	pure p			

Natural Bond Orbital Analysis of the Compounds 2h, 9, 11, and 12. The natural bond orbital (NBO) analysis[16] of the Dewar isomer **2h**, 2-azetidinone **9**, dihydroazete **11**, and straight-chain imines **12** gives some reasonable results. The hybridization factors of the compounds **2h**, **9**, **11**, and **12** are shown in Table 7. The hybridization characters of the N6 atom and its lone pair in the 2-azetidinone derivatives **2h** and **9** are close to sp^2 and pure p character. The p character contributions to the endocyclic C1−N2, N2−C3, and C3−C4 bonds in **11** are larger than those in (*Z*)-**12** (Table 7). The s character contributions to the exocyclic C3−H bond and N2 lone pair in **11** is much larger than those of the C3−H bond and N2 lone pair of the (*Z*)-**12**. The reductions of the bond angles (C1−N2═C3 and C4−C3═N2) by cyclization from the (*Z*)-imine **12** to the cyclic imine **11** are responsible for increase of p character in the endocyclic bonds (C1−N2, N2−C3, and C3−C4) and for increase of s character in the exocyclic C3−H bond and of the N2 lone pair. Similarly, the bridgehead C1 and C4 atoms of the Dewar **2h** have greater p character in the C1−C4 bond and greater s character in the C1−H and C4−H bonds than those in the corresponding bonds of the 2-azetidinone **9** and dihydroazete **11** (Table 7). The properties of the bond characters in the bicyclic Dewar **2h** are due to the smaller N6−C1−C4 (89°) and C5−C4−C1 (85°) bond angles in **2h** than the H1′−C1−C4 (115−116°) and H4′−C4-C1 (116°) bond angles in the monocyclic compounds **9** and **11** (Figure 8). The greater p orbital contribution of the C1 and N2 atoms in the cyclic compounds **2h** and **11** may lengthen the bond distance of the C1−N2 bond than that of straight-chain imines **12** since p orbital extension is larger toward bond direction than s orbital extension.

(25) Abboud, J.-L.; Canada, T.; Homan, H.; Notario, R.; Cativiela, C.; Diaz de Villegas, M. O.; Bordeje, M. C.; Mo, O.; Yanez, M. *J. Am. Chem. Soc.* **1992**, *114*, 4728−4736.
(26) Bachrach, S. M.; Liu, M. *J. Org. Chem.* **1992**, 57, 209−215.
(27) (a) Wiberg, K. B.; Nakaji, D. Y.; Morgan, K. *J. Am. Chem. Soc.* **1993**, *115*, 3527−3532. (b) Wiberg, K. B.; Glaser, R. *J. Am. Chem. Soc.* **1992**, *114*, 841−850.

Charge Distributions and Bond Orders of the Compounds 2d, 2h, 9, 11, and 12. The charges by the natural population analysis (NPA)[16] of the Dewar pyrimidinones **2d** and **2h**, 2-azetidinone **9**, dihydroazete **11**, and straight-chain imines **12** are shown in Table 3S (Supporting Information). The charge distribution of the (*E*)-imine **12** is almost the same as that of the (*Z*)-imine **12**. Then, the charge distribution of the (*Z*)-imine **12** is used for comparison with the related compounds (Figure 9). The variation of charge on the N2 and C3 atoms between the cyclic imine **11** and (*Z*)-imine **12** is quite small (0.035e−0.037e) and that of hydrogen atoms is negligibly small (ca. 0.004e on the average). The amount of negative charge on the C1 and C4 atoms of **11** is smaller by ca. 0.20e−0.22e than those of the (*Z*)-imine **12.** The decreased amount of negative charge on the C1 and C4 atoms in **11** is approximately equal to the amount of positive charge (+0.21e−+0.24e) on the methyl hydrogen atom at the C1 and C4 positions in the (*Z*)-imine **12**. The replacement of hydrogens in the Dewar **2h** by methyl groups at the C1, C3, and N6 atoms increases positive charge on the C1 and C3 atoms by ca. 0.21e and decreases negative charge on the N6 atom by 0.18e in the Dewar **2d**. The difference of positive charge on the C1 and C3 atoms between **2d** and **2h** is approximately equal to the amount of positive charge (+0.22e−+0.24e) on the H1 and H3 atoms of **2h**. The amounts of charge on the N2, C4, C5, O9, and H4 atoms vary in the range from 0.034e to 0.004e between **2d** and **2h** and are much smaller than those on the C1 and C3 atoms. The replacement of the C−H bond by the C−C bond gives variation of charge on the carbon atom. The results can be explained by assuming additivity of separated charge on the atom. The formation of the homopolar C−C bond corresponds to reduction of polarization originated from the C−H bond. The methyl group on the N6 position in **2d** gives smaller negative charge on the N6 atom than that of **2h** because the methyl carbon atom in **2d** is more electronegative than the H6 hydrogen atom in **2h** and withdraws more negative charge from the N6 atom. The charge on the C1 atom bonded with the one electronegative N2 or N6 atom is negative (−0.20e to −0.45e) in the compounds (**9**, **11**, and **12**). The two electronegative N2 and N6 atoms give positive charge on the C1 atom (+0.18e−+0.38e) in the bicyclic Dewars (**2d** and **2h**). The methyl substitution, cyclization, and fusion of the dihydroazete with the 2-azetidinone ring give significant increase of positive charge on the C1 atom of the trimethyl Dewar **2d**.

The AIM (atoms in molecules)[28] bond orders of the Dewar **2h**, 2-azetidinone **9**, dihydroazete **11**, and straight-chain (*E*)-imine **12** are summarized in Table 4S (Supporting Information).[29] Unlike the AIM bond order of 2.0 for ethylene,[28b] the bond orders of the N2═C3 for the Dewar and imines **2h**, **11** and **12** and of the C5═O9 for the Dewar isomer and 2-azetidinone **2h** and **9** are ca. 1.6 and 1.3, respectively. The results reflect the polar characters of the double bond.[28b] The NPA atomic charge distributions confirm this description such as the N2 (−0.480e)═C3 (+0.131e) and C5 (+0.855e)═O9 (−0.672e) bonds in **2h** (Figure 9). The AIM bond orders of the six single bonds (C1−N2, C1−C4, C1−N6, C3−C4, C4−C5, and C5−N6) for the compounds **2h**, **9**, **11**, and **12** are from 0.99 to 0.88 and are close to the AIM C−C bond order of 1.05 for ethane.[28b] The C1−N2 bond order (0.93) of the Dewar **2h** is nearly the same as those (respectively, 0.95 and 0.96) of the cyclic imine **11** and straight-chain (*E*)-imine **12**, indicating little or no effect on the bond orders of the compounds **2h**, **9**, and **11** by cyclization and fusion with the 2-azetidinone and dihydroazete moieties.

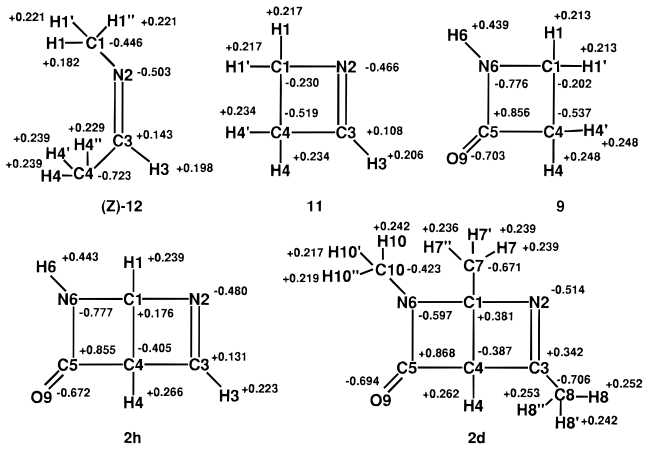

Figure 9. Atomic charges by natural population analysis (NPA) of the Dewar pyrimidinones **2d** and **2h**, 2-azetidinone **9**, dihydroazete **11**, and (*Z*)-imine **12** at the MP2/6-31G(d,p) level of theory.

Conclusions

The abnormal C1−N2 bond lengthening in the Dewar pyrimidinones **2** is unambiguously confirmed by the X-ray structure determination and theoretical calculations. Furthermore, the ab initio molecular orbital calculations elucidate the significant charge separations and increase of p-character in the endocyclic bonds. The unusual ionic C1−N2 bond cleavage of the 1,3,6-trialkyl Dewar pyrimidinones **2** in the protic solvents can be qualitatively understood in terms of the abnormally longer C1−N2 bond distance, enormous positive charge on the C1 atom, and great p character in the C1−N2 bond.

Acknowledgment. The authors thank Professor H. Hongo (Tohoku College of Pharmacy) for providing the X-ray structure data of the Dewar pyridone **8b**.

Supporting Information Available: Tables (1S−14S) of the X-ray least-squares planes of the Dewar **2a**−**c**, selected bond distances and angles of the compounds **9**, **11**, and **12**, atomic charges of the compounds **2d**, **2h**, **9**, **11**, and **12** by the natural population analysis (NPA), AIM bond orders of the compounds **2h**, **9**, **11**, and (*E*)-**12** by the theory of atoms in molecules (AIM), and Cartesian coordinates [MP2/6-31G(d,p)] for the Dewar pyrimidinones **2a**,**d**−**h**, 2-azetidinone **9**, dihydroazete **11**, and imines **12** (17 pages). This material is contained in libraries on microfiche, immediately follows this article in microfilm version of the journal, and can be ordered from the ACS; see any current masthead pages for ordering information.

JO962103Z

(28) (a) Bader, R. F. W. Atoms in Molecules−A Quantum Theory; Oxford: London, 1991. (b) Cioslowski, J.; Mixon, S. T. *J. Am. Chem. Soc.* **1991**, *113*, 4142−4145.

(29) (a) The bond orders of the compounds **2h**, **9**, **11**, and (*E*)-**12** by the AIM theory using optimized MP2/6-31G(d,p) wave functions were computed on a Sun SPARCstation20. (b) The AIM calculations of the Dewar **2d** and (*Z*)-imine **12** were unsuccessful.

(30) Tables of complete atomic positional parameters with equivalent isotropic factors, anisotropic displacement parameters, bond distances, bond angles, torsion angles, and observed and calculated structure factors for **2a**−**c** have been deposited with Cambridge Crystallographic Data Centre. This material can be obtained from the Director, Cambridge Crystallographic Data Centre, 12 Union Road, Cambridge, CB2 1EZ, UK.